Proceedings of the ASME 2017 36th International Conference on Ocean, Offshore and Arctic Engineering June 25-30, 2017, Trondheim, Norway

OMAE2017-61292

DYNAMIC SIMULATION AND CONTROL OF AN ACTIVE ROLL REDUCTION SYSTEM USING FREE-FLOODING TANKS WITH VACUUM PUMPS

Jiafeng Xu

Centre for Research-based Innovation Centre for Research-based Innovation Centre for Research-based Innovation on Marine Operations (SFI MOVE) Department of Ocean Operations and Civil Engineering Norwegian University of Science and Technology, NTNU NO-6009 Aalesund, Norway Email: jiafeng.xu@ntnu.no

Zhengru Ren

on Marine Operations (SFI MOVE) Centre for Autonomous Marine Operations and Systems (AMOS) Department of Marine Technology Norwegian University of Science and Technology, NTNU NO-7491 Trondheim, Norway Email: zhengru.ren@ntnu.no

Yue Li

on Marine Operations (SFI MOVE) Department of Ocean Operations and Civil Engineering Norwegian University of Science and Technology, NTNU NO-6009 Aalesund. Norway Email: yue.li@ntnu.no

Roger Skjetne

on Marine Operations (SFI MOVE) Centre for Autonomous Marine Operations and Systems (AMOS) Department of Marine Technology Norwegian University of Science and Technology, NTNU NO-7491 Trondheim, Norway Email: roger.skjetne@ntnu.no

Karl Henning Halse

Centre for Research-based Innovation Centre for Research-based Innovation on Marine Operations (SFI MOVE) Department of Ocean Operations and Civil Engineering Norwegian University of Science and Technology, NTNU NO-6009 Aalesund, Norway Email: karl.h.halse@ntnu.no

ABSTRACT

Ship roll motion is often the critical factor for offshore operations due to its lack of damping mechanism. This paper demonstrates a dynamic simulation scheme of an active roll reduction system using free-flooding tanks controlled by vacuum pumps. The two tanks in the system are installed on each sides of a catamaran. The tank hatches are opened to the sea and the air chambers of both tanks are connected by an air duct. Vacuum pumps and air valve with active stabilization controller provides desired filling level for the tank. The ship is a dynamic model with single degree of freedom in roll. The hydrodynamic behavior of the ship is calculated using potential theory by SHIPX. The air chamber above is modelled as isothermal process of ideal gas. The behavior of the liquid flow in the tank is simulated by incompressible RANS solver using Volume of Fluid (VOF) model, then summarized as response function for the ship model. A simplified control plant model for the vacuum pumps is proposed where insignificant higher order behaviors are regarded as biases and noises. The stability is proved by Lapunov direct method. The performance of the entire system is evaluated in terms of roll reduction capability and power cost. The system is more suitable for roll reduction in low-speed or resting conditions.

INTRODUCTION

Ship roll motion is often the critical factor for offshore operations due to its lack of damping mechanism. Excessive roll motion could cause both physiological and psychological issues such as acceleration induced fatigue and cognitive impairment, as well as engineering issues such as structural failure and cargo damage. Passive roll reduction methods such as bilge keel, fixed fins, free-surface tank, and U-tank have proved their own strengths and weaknesses in numerous studies [1,2]. Active roll reduction methods such as active fins and pneumatic/hydraulic pump activated tanks are studied in [3,4]. This paper revisits the concept of free-flooding tanks with pneumatic pump. The dynamic system is modelled with more nonlinear characteristics and the control system is a model-based design.

Frahm [5] first introduced the U-tank as an improvement to the many disadvantages of free-surface tank. Based on Frahm's work, some modifications have removed the horizontal water channel on the bottom of the U-tank. As a result, the bottoms of the tanks are opened to the sea [4]. These so-called "freeflooding tanks" have been retrofitted to six USN cruisers of Pensacola and Northampton classes during 1931-1932 and later in 1988 to the aircraft carrier USS Midway. The air chambers on the top of each tank were connected by air duct and controlled by valve and air pump. More recently a Norwegian company Marine Roll & Pitch Control(MRPC) proposed a design where the air chambers of two tanks are isolated and controlled by individual pumps separately [6]. The design of free-flooding tanks are ideally suitable for multi-hulls like catamarans or trimarans which have a longer level arm and subsequently less required volume for tanks. On the downside, the free-flooding tanks are susceptible to high cruising speed since the effective water inlet will be reduced.

The target system in this paper is a catamaran with one free-flooding tank installed on each side. The tank hatches are opened downwards into the sea. The air duct on top of the chamber is connected to a vacuum pump. The pump is part of a larger control system which will control the air flow to both tanks. The inlet flow from one side is not necessarily equal to the outlet flow to the other side due to the requirement of pressure level in both tanks. The design is similar to the classical "N-tank" proposed by Bell & Walker [4]. Moaleji [7] modelled the system in a rather hydrostatic perspective and proposed an adaptive inverse controller. This paper tries to add more hydrodynamic feature into the dynamic model and propose a model-based controller.

MATHEMATICAL MODELLING Tank

The tanks used in this model are simplified as two cuboids with a constant cross section profile and a hatch opening on the bottom. The hatch is considered to be a sharp-edged orifice. The flow rate across the hatch can then be expressed as basic turbulent

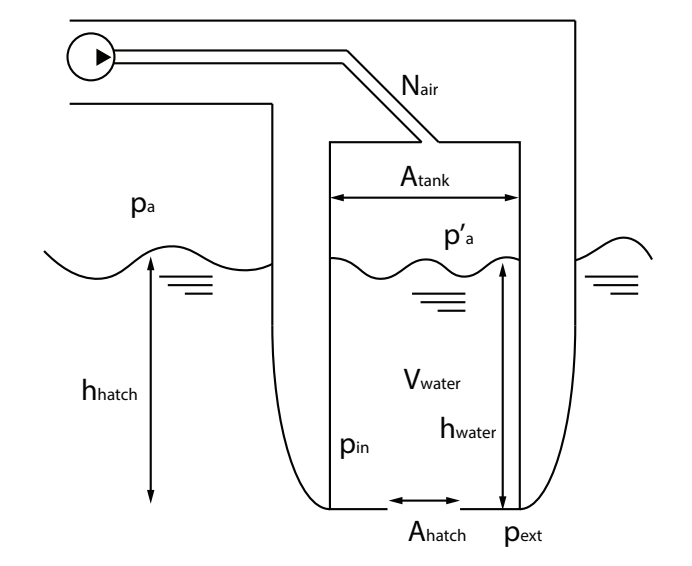


FIGURE 1. FREE-FLOODING TANK ON A CATAMARAN

flow model:

$$\dot{V}_{water} = C_d \cdot A_{hatch} \sqrt{\frac{2}{\rho} \cdot \Delta p}, \tag{1}$$

where Δp is the pressure difference between either side of the hatch, and C_d is the discharge coefficient. Traditionally, C_d can be found around 0.6-1.0 for nozzles and orifices in a fluid system depending on their configurations and dimensions. However, the inlet/outlet flow across the hatch is periodic and the wave period is too short for a fully developed flow inside the tank. Hence, necessary CFD calculations are carried out using Star CCM+.

First, the CFD study is carried in 2D and separated into two distinctive processes: inlet and outlet. The air inside the tank is treated as an ideal gas, while the water is an incompressible fluid. Multiphase flow is modelled using Volume of Fraction. Turbulence is modelled by standard K-Epsilon model. Assuming the external pressure is constant, the varying pressure difference and the hatch opening ratio have been studied and compared. Fig. 2 is an example of hatch area ratio 0.2 with 0.9 meters water head pressure difference.

For outlet flow, no obvious vortex is detected. C_d holds a value around 0.8 for a variety of settings; see Fig. 3. Hence, in the model, C_d is set as constant for outlet flow. In terms of inlet flow, two apparent vortices are detected in the vicinity of the hatch; see Fig. 4. This will create extra low pressure areas; see Fig. 5. In the mathematical model, the internal pressure of the tank is calculated from the water head of the tank as in Eqn. (3), so that the extra pressure difference caused by vortices are compensated by an inflated C_d of 1.5.

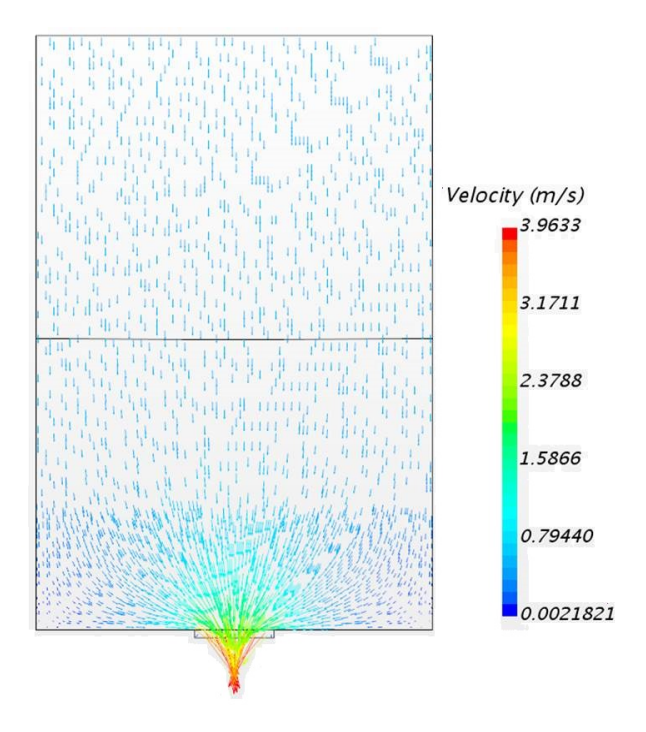


FIGURE 2. VELOCITY FIELD OF OUTLET FLOW

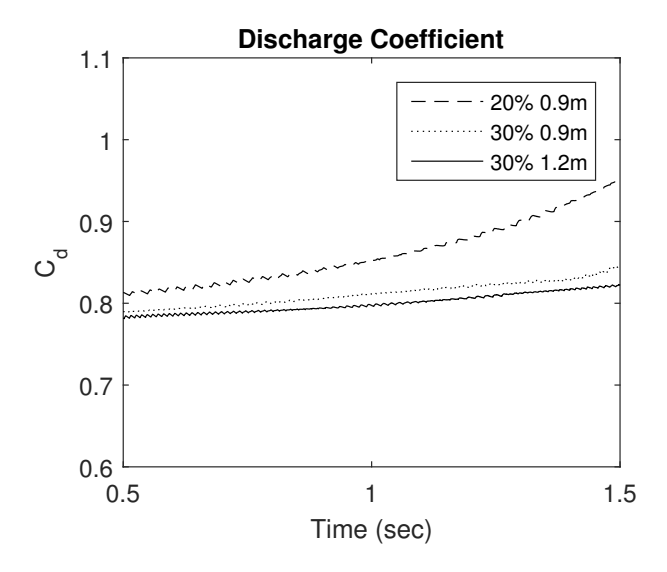


FIGURE 3. DISCHARGE COEFFICIENT

The CFD calculation is then conducted in 3D. A square shape hatch and a round shape hatch with the same characteristic length (edge equals diameter) are studied. The dimension of the cuboid tank is the same as in 2D study. Figure 6 shows the velocity distribution on the water surface during inlet flow. Figure 7 shows the comparison of discharge coefficient with square and round shape hatches. The 3D results match the 2D results

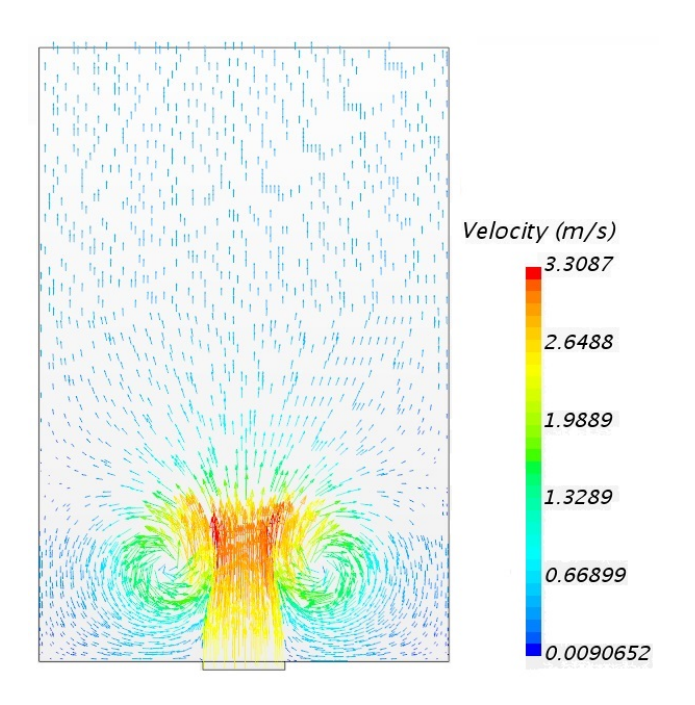


FIGURE 4. VELOCITY FIELD OF INLET FLOW

quite well, so that the assumption of C_d made in the 2D analysis seems still valid. It is important to emphasize that the model is still under strong linear approximation. C_d chosen here are time average values of the steady state. More realistic models need to be made under deeper study of the hydrodynamics, and ideally CFD calculations shall be included in the simulation loop directly without any fitting or statistics.

The calculation of external pressure derives from Bernoulli's equation and consists of three components: the time variant dynamic pressure of waves, hydrostatic pressure, and atmospheric pressure

$$p_{ext} = \frac{\partial \Phi}{\partial t} + \rho \cdot g \cdot h_{hatch} + p_a. \tag{2}$$

The pressure drop due to hatch velocity is neglected because the local fluid flow is a complex fluid-structure interaction for which the pressure drop may be compensated by structure drag. Any further assumptions become groundless without comprehensive CFD calculations. The internal pressure of the hatch consists of two components: the internal hydrostatic pressure, and compressed or expanded internal air pressure. This is given by

$$p_{in} = \rho \cdot (g - y \cdot \ddot{\phi}) \cdot h_{water} + p'_{a}. \tag{3}$$

The internal hydrostatic pressure uses a variable acceleration term due to the weightlessness caused by the roll acceleration

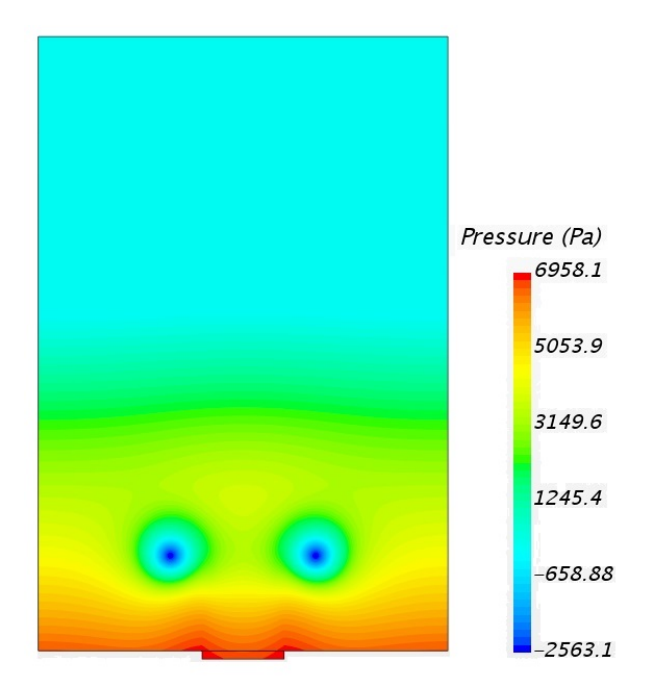
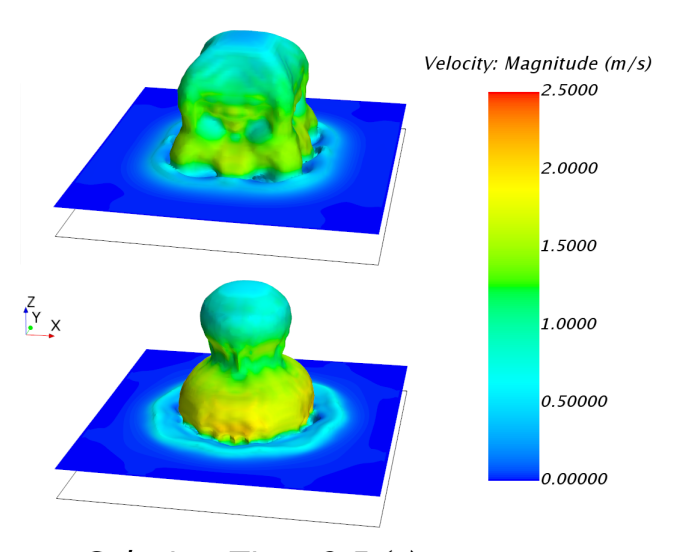


FIGURE 5. PRESSURE FIELD OF INLET FLOW



Solution Time 0.5 (s)

FIGURE 6. WATER SURFACE UNDER INLET FLOW

of the vessel, which explains the use of y as lateral leveling arm of the tank in Eqn. (3). However, this would cause the entire state equation of the system to become implicit. The internal air is assumed under the isothermal process of ideal gas. For a given initial pressure p_{init} and volume V_{init} , and the air transfer $N_{air}\{kg.m2/s2\}$ in and out of the tank, the internal air pressure

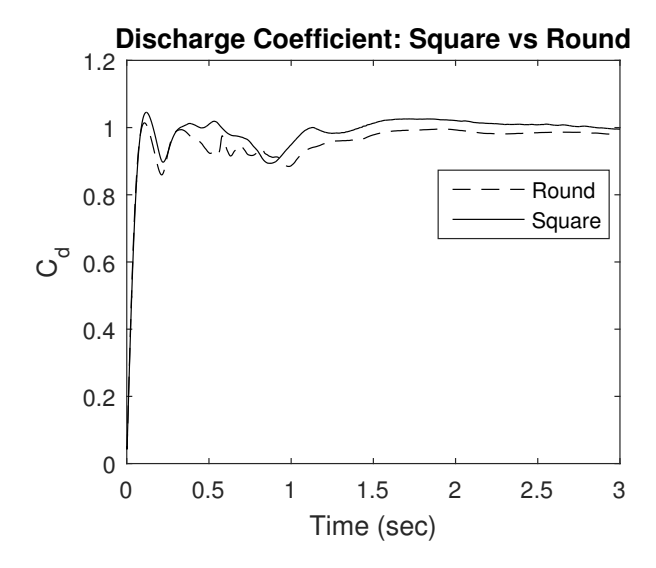


FIGURE 7. DISCHARGE COEFFICIENT: SQUARE VS ROUND

at any given moment is

$$p_a' = \left(\int_{t_0}^t \dot{N}_{air}\right) / \left(V_{tank} - V_{water}\right). \tag{4}$$

Pump

The vacuum pump is modelled as a linear system without time delay and with a maximum power output. Since the pump does not always pump the air from low pressure side to high pressure side, some portion of the air transfer happens passively. The passive air transfer is controlled by a valve using the same principle of an orifice as in Eqn. (1)

$$\dot{N}_{passive} = C_d \cdot A_{valve} \sqrt{2\rho \cdot \Delta p}, \tag{5}$$

where Δp is the pressure difference of two sides of the valve and C_d is approximated as 0.6 although more complex models exist in other works which focus on the internal details of the pump [8]. The extra air transfer required will be provided by the pump. The effective power required for pump can be calculated from air transfer rate as

$$P_{pump} = (\dot{N}_{air} - \dot{N}_{passive}) \cdot \Delta p / p_{in}, \tag{6}$$

where p_{in} is the pressure on the inlet side.

Vessel

The target catamaran is simplified as a single degree-of-freedom roll model. The governing equation is

$$(I + I_{A}(\infty) + \Delta I) \cdot \ddot{\phi}(t) + D(\infty) \dot{\phi}(t) + \int_{0}^{t} K(t - \tau) \dot{\phi}(t) d\tau + T \cdot \phi(t) = \tau_{wave}(t) + \tau_{tank}(t),$$
(7)

where I, $I_A(\infty)$, ΔI , and ϕ are moment of inertia, added moment of inertia, the varying moment of inertia due to the loss/gain of the water in the tanks, and rolling angle of the vessel, respectively, $D(\infty)$ is the linear damping coefficient, K(t) is the fluid-memory effect [9], which is formulated by a state-space model [10]. T is the linear restoring torque coefficient, $\tau_{wave}(t)$, $\tau_{tank}(t)$ are the torques exerted by the wave and the loss/gain of buoyancy from tanks on both sides. The internal fluid is considered bounded by the tank sides and moving with the vessel. Hydrodynamics related coefficients are generated from strip theory in SHIPX.

CONTROL ALGORITHM

Problem Formulation

The control algorithm is based on a simplified model where insignificant higher order behaviors are regarded as biases and noises. The simplified model is summarised in Eqn. (8).

$$\dot{\phi} = p,\tag{8a}$$

$$\dot{p} = \frac{1}{L}(-T\phi - D\dot{\phi} + \tau_{tank} + d), \tag{8b}$$

$$\dot{V}_{w1} = C_{v1} \operatorname{sgn}(\Delta P_{h1}) / \sqrt{|\Delta P_{h1}|}, \tag{8c}$$

$$\dot{V}_{w2} = C_{v2} \operatorname{sgn}(\Delta P_{h2}) / \sqrt{|\Delta P_{h2}|}, \tag{8d}$$

$$\dot{N}_{a1} = u_1, \tag{8e}$$

$$\dot{N}_{a2} = u_2, \tag{8f}$$

where p is an alias for roll velocity; T,D are the linearized restoring and damping coefficient; I_t is the total moment of inertia of the catamaran; $C_{vt} = C_{d_t} A_{hatch_t} \sqrt{2/\rho}$ is the combined discharge coefficients, where $t \in \{1,2\}$ are tank indices; ΔP_{ht} is pressure difference around hatch; $\dot{N}_{at} = u_t$ is the air transfer rate; d represents the slowly-varying state including all sorts of bias, such as weightlessness effect in Eqn. (3), fluid-memory effect and the moment of inertia variation of the tank in Eqn. (7).

The block diagram of the closed-loop system is presented in Fig. 8. The plant can be regarded as a cascade which is closed by control. The control objective is to regulate the roll angle to zero, i.e., $\phi(t) \to 0$ as $t \to \infty$. A parameter-dependent observer is applied to estimate the external disturbance. Then the external disturbance is compensated in the backstepping process. A

command signal is generated as the output of the backstepping control law. Then,a PID controller is used to track the command, i.e., $\tau_{tank}(u_1(t), u_2(t)) \rightarrow \tau_{tank}^{cmd}(t)$. The following assumptions are made:

- 1. The volumes of the tanks are much smaller than the vessel. Therefore we consider the total moment of inertia I_t is a constant with a rough initial estimate.
- An exosystem is assumed to be suitable to approximate the external disturbance.
- 3. The parameter-dependent observer does not monitor the frequency nor the amplitude of the wave. Hence the system has tolerance to irregular waves.

Lemma 1 ([11]). Consider the dynamic system $\dot{\zeta} = G\zeta + bd$, where $\zeta \in \mathbb{R}^q$ is the state, the pair (G,b) is controllable. Then, for any Hurwitz matrix $G \in \mathbb{R}^{q \times q}$, there exists a unique constant vector $\psi \in \mathbb{R}^1$, s.t., the disturbance d can be expressed in the form $d = \psi^\top \zeta + \psi^\top \delta_d$, and $\dot{\delta}_d = G\delta_d$.

Lemma 2 (Rayleigh-Ritz theorem [12]). *If the matrix* $A \in \mathbb{R}^{n \times n}$ *and the vector* $x \in \mathbb{R}^n$ *are real, then*

$$\lambda \|x\|^2 < z^{\top} A z < \overline{\lambda} \|x\|^2, \tag{9}$$

where $\underline{\lambda}(Q)$ and $\overline{\lambda}(Q)$ are the smallest and largest eigenvalues of A.

Parameter-dependent Observer

Based on the famous Internal Model Principle (IMP), reference signal or external disturbances can be asymptotically tracked if the external generator model is suitably reduplicated in the feedback path of the closed-loop control system [11]. The exosystem is given by

$$\dot{\chi} = \Gamma \chi, \tag{10a}$$

$$d = l^{\top} \chi, \tag{10b}$$

where $\chi \in \mathbb{R}^q$ is the state of the exosystem, and (Γ, l^\top) is assumed to be observable. Assume q is known, Γ and l are unknown, and χ and d are not measurable.

A second-order exosystem is used to estimate the disturbance, i.e., q=2. The parameter-dependent observer is given by

$$d = \vartheta^{\top} \xi + \psi^{\top} \delta, \tag{11a}$$

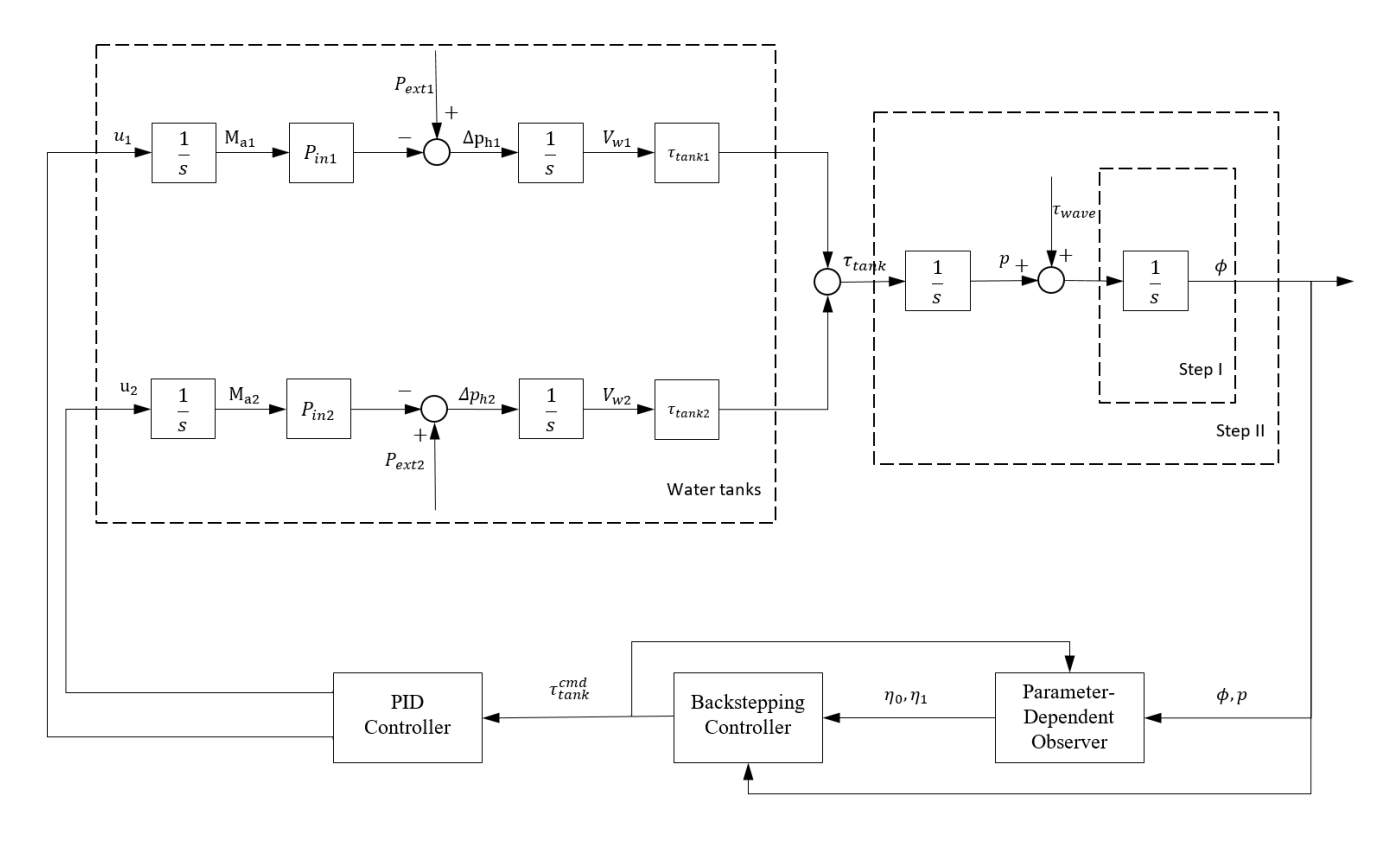


FIGURE 8. BLOCK DIAGRAM OF THE FOUR-STEP BACKSTEPPING CONTROLLER

where

$$\vartheta = [\boldsymbol{\psi}^{\top}, \boldsymbol{\theta}_1 \boldsymbol{\psi}^{\top}]^{\top}, \tag{11b}$$

$$\boldsymbol{\xi} = [(\boldsymbol{\eta}_0 + \boldsymbol{v})^\top, \boldsymbol{\eta}_1^\top]^\top, \tag{11c}$$

$$\dot{\eta}_0 = G\eta_0 + Gv(x) - bu, \tag{11d}$$

$$\dot{\eta}_1 = G\eta_1 - \psi_1,\tag{11e}$$

$$b = [0, 1]^{\top}, \ v(x) = [0, v_2]^{\top}, \ v_2 = I_t p.$$
 (11f)

The total control effort τ_{tank}^{cmd} is splitted into two parts,

$$\tau_{tank}^{cmd} = u_{v} + u_{d}, \tag{14}$$

where u_y responses to the path following, and u_d counteracts the disturbance d.

Step I: Select the control Lyapunov function as $V_1 = \frac{1}{2}z_1^2$, and let

$$\alpha_1 = -c_1 z_1, \tag{15}$$

where c_1 is a positive gain constant. Substitute Eqn. (8a) and Eqn. (15) into V_1 , yields

$$\dot{V}_1 = -c_1 z_1^2 + z_1 z_2. \tag{16}$$

Then,

$$\dot{z}_1 = -c_1 z_1 + z_2. \tag{17}$$

Backstepping

Backstepping is a recursive control design for systems in strict feedback form [13, 14]. The design process is illustrated as follows. Define two new states

$$z_1 := \phi, \tag{12}$$

$$z_2 := p - \alpha_1, \tag{13}$$

where α_1 is a vertial control.

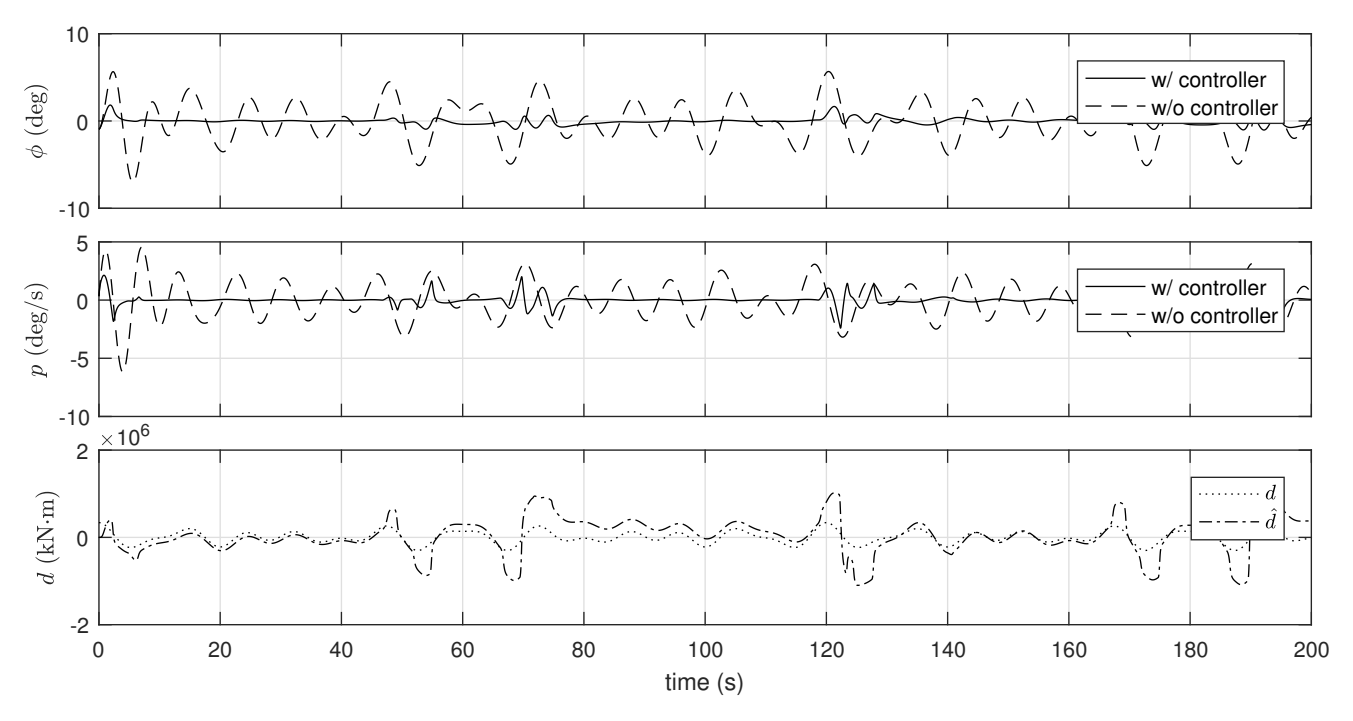


FIGURE 9. CONTROLLER PERFORMANCE ($Hs = 3.6m, L_{tank} = 15m$)

Step II: Substitute Eqn. (8b) into the time derivative of Eqn. (13), yields a new error state equation, which is given by,

$$\dot{z}_2 = \frac{1}{I_t} (-T\phi - Dp + d + u_y + u_d) - \dot{\alpha}_1.$$
 (18)

Construct a new control Lyapunov function,

$$V_2 = V_1 + \frac{1}{2}z_2^2. (19)$$

Differentiate Eqn. (19) and substituting Eqn. (18) yields,

$$\dot{V}_2 = -c_1 z_1^2 + z_2 [z_1 + \frac{1}{L} (-T\phi - Dp + d + u_y + u_d) - \dot{\alpha}_1]. \quad (20)$$

Choose a virtual control as

$$u_v = T\phi + Dp + I_t(-z_1 + \dot{\alpha}_1 - c_2 z_2),$$
 (21)

where c_2 is a positive gain constant. Substitute Eqn. (11a) and (21) into Eqn. (18) yields,

$$\dot{z_2} = -z_1 - c_2 z_2 + \frac{1}{I_t} (\vartheta^{\top} \xi + \psi^{\top} \delta + u_d).$$
 (22)

Then, u_d is designed as

$$u_d = -\hat{\vartheta}^{\top} \xi - \frac{z_2}{L}. \tag{23}$$

The adaptation law is chosen as

$$\dot{\hat{\vartheta}} = \frac{k_1}{I_t} \xi z_2,\tag{24}$$

where $k_1 > 0$ is the design parameter. Substitute Eqn. (23) into Eqn. (22), yields,

$$\dot{z_2} = -z_1 - c_2 z_2 + \frac{1}{I_t} (\tilde{\vartheta}^{\top} \xi + \psi^{\top} \delta - \frac{z_2}{I_t}).$$
 (25)

Theorem 3. Consider the closed-loop system consisting of the plant (8a)-(8b), uncertain exosystem (10), parameter-dependent observer (11), and adaptive regulator (21), (23), and (24) can stabilize the system $\phi \to 0$, as $t \to \infty$.

Proof. Define the error state, $\tilde{\vartheta} = \vartheta - \hat{\vartheta}$. As ϑ is assumed to be constant; therefore, $\dot{\tilde{\vartheta}} = -\dot{\hat{\vartheta}}$. Choose the Lyapunov function as

$$V = \frac{1}{2}z_1^2 + \frac{1}{2}z_2^2 + \frac{1}{2k_1}\tilde{\vartheta}^\top\tilde{\vartheta} + k_\delta \delta^\top P \delta, \tag{26}$$

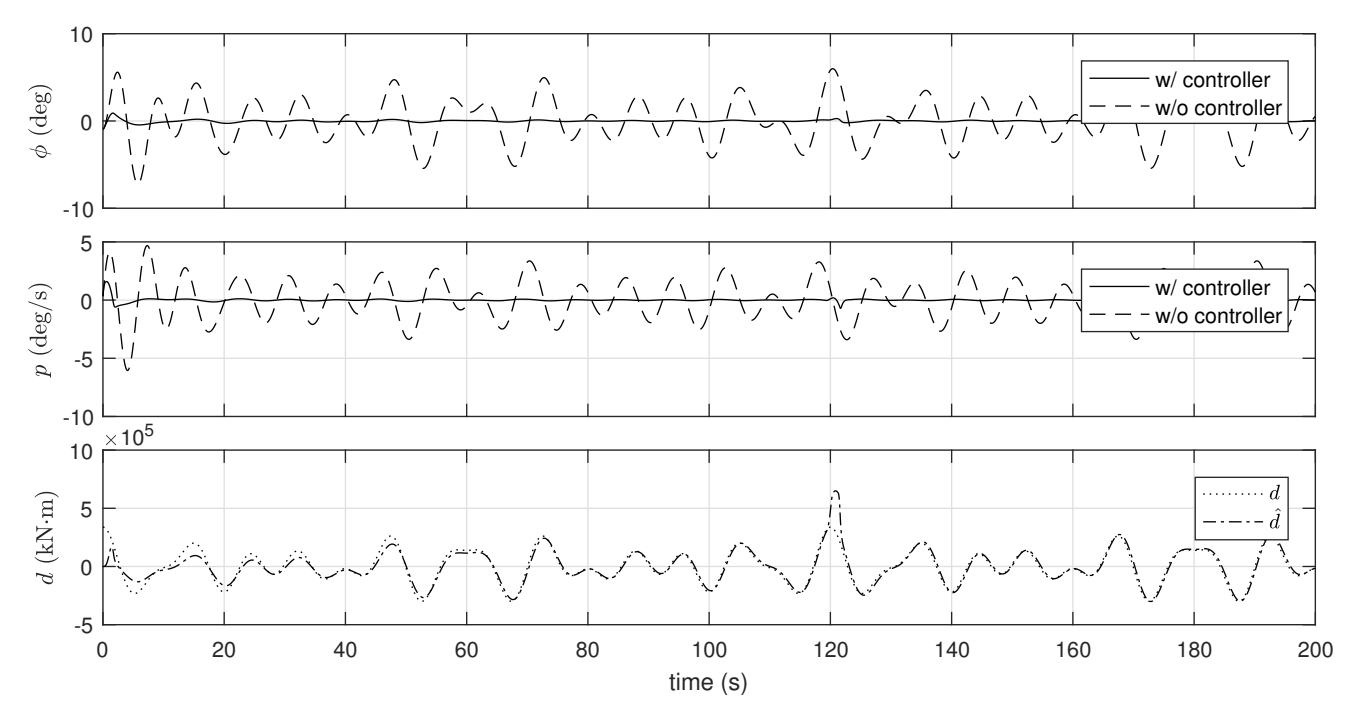


FIGURE 10. CONTROLLER PERFORMANCE ($Hs = 3.6m, L_{tank} = 20m$)

where $P = P^{\top} > 0$ satisfying $G^{\top}P + PG = -I$, and k_{δ} is larger than the maximum eigenvalue of the matrix $\psi\psi^{\top}$. Taking the time derivative of Eqn. (26), using Lemma 1 and Lemma 2 leads to

$$\begin{split} \dot{V} &= -c_1 z_1^2 - c_2 z_2^2 + \frac{z_2}{I_t} \tilde{\vartheta}^\top \xi - (\frac{z_2}{I_t})^2 + \frac{z_2}{I_t} \psi^\top \delta \\ &- \frac{1}{k_1} \tilde{\vartheta}^\top \dot{\hat{\vartheta}} + k_\delta \delta^\top (G^\top P + PG) \delta \\ &= -c_1 z_1^2 - c_2 z_2^2 - (\frac{z_2}{I_t})^2 + \frac{z_2}{I_t} \psi^\top \delta - k_\delta \delta^\top \delta \\ &\leq -c_1 z_1^2 - c_2 z_2^2 - (\frac{z_2}{I_t})^2 + \frac{z_2}{I_t} \psi^\top \delta - (\delta \psi^\top)^2 \\ &\leq -c_1 z_1^2 - c_2 z_2^2 - \frac{3}{4} (\psi^\top \delta)^2 \leq 0. \end{split}$$

When $\dot{V}=0$, $z_1=\dot{z}_1=z_2=\dot{z}_2=\psi^\top\delta=0$. From Eqn. (25), $\tilde{\vartheta}$ has to be zero, if $\xi\neq0$. From LaSalle-Yoshizawa theorem [13], every solution starting in $\{\Omega|\dot{V}=0\}$, therefore, $z_1\to0$, as $t\to\infty$.

NUMERICAL EXAMPLE

To analyze the dynamic behavior of the entire system and its control algorithm, a numerical example is set up in this section. Instead of having a realistic parameter set, the parameters are chosen to serve a plausible starting point for the preliminary design. A catamaran with one tank on each side is studied. The main parameters of the system are in Table 1. The system can provide its maximum counter torque when the tank on one side is completely emptied and the other one is full.

Controller Performance

After a fine tuning process, Fig. 9, 10, and 11 show the time domain simulations under different significant wave heights and tank lengths. The first two subplots show the vessel motion and velocity with and without the anti-roll controller. The third subplot shows the disturbance predicted by the observer comparing with the actual value. The wave spectrum has three main frequency components. More components require a higher order configuration of the observer. Figure 9 shows that with insufficient maximum tank volume, the system cannot fully compensate the wave-induced vessel motion. The observer can estimate the wave-induced disturbance quite well after some starting time, but once the system capacity is overloaded, the observer needs time to re-converge. Fig. 10 shows an improved performance after the tank length is increased from 15m to 20m. The controller largely reduces the amplitude of the roll motion. During the simulations, the influence of the changing moment of inertia caused by the tanks are not remarkable. Fig. 11 shows for severe wave condition, an even larger tank is still theoretically possible. But an over-sized anti-roll tank will surely cause other design problems. Note that the roll reduction is not perfect. Increasing the

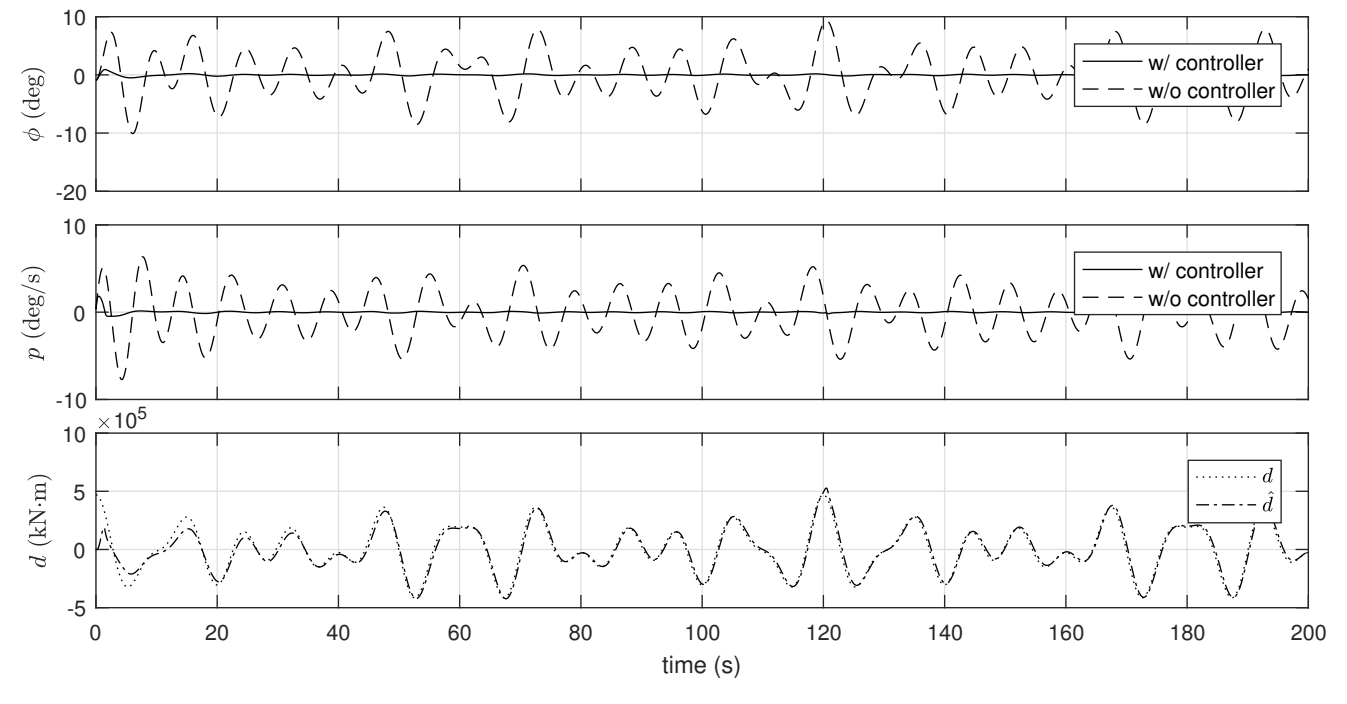


FIGURE 11. CONTROLLER PERFORMANCE (Hs = 5m, $L_{tank} = 30m$)

Vessel Length	100 m
Vessel Breadth	42 m
Vessel Depth	11 m
Vessel Draft	9 m
Vessel Mass	19345 ton
Vessel Roll Moment of Inertia	3e9 kg.m2
Wave Height	2 m
Wave Period	5 - 12 sec
Tank Length, Width and Height	(15-30)x8x8 m
Tank Torque Arm	24 m
Hatch Area	15 m2
Valve area	1 m2
Pump Max. Power	300 kW

TABLE 1. SYSTEM MAIN PARAMETERS

control gains in the backstepping and PID controllers are helpful to make the control more responsive; However, the control gains directly determined by the control cost and physical capability of the actuators.

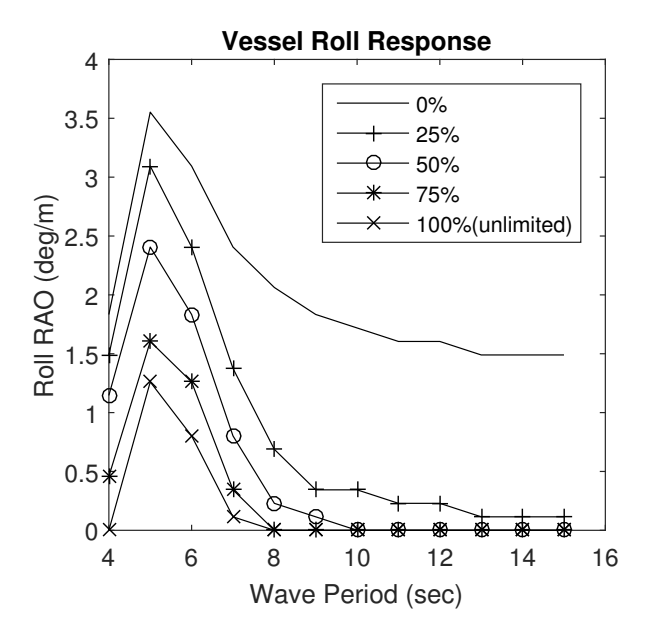


FIGURE 12. VESSEL ROLL RESPONSE ($H = 2m, L_{tank} = 20m$)

Pump Capacity

Figure 12 shows the vessel roll response in frequency domain under different pump capacity. The 100% line is actually conducted with unlimited pump power.

The target catamaran has a very low natural period of roll

due to its large breadth. Even with unlimited power, the system cannot fully compensate the wave induced roll motion. Also the smaller the wave period is, the higher the energy it carries, and less action time is available for the system. As the wave period increases, the effect of the proposed anti-roll system improves, resulting in a greater amplitude reduction from uncontrolled motion.

There are many other parameters that significantly influence the simulation result and the efficiency of the entire system. If the hatch area is too small, greater pressure difference around the hatch is required to achieve the desired water flow, which can only be achieved by having a more powerful pump to create greater air pressure change in a certain time period. If the hatch is too big, despite the increasing structural vulnerability, the passive movement of tank waters may be out of phase with the vessel motion, causing a decreased capability of passive control and increased demand for active pump power. The same principle applies to the design of air duct and valve; the diameter of the duct and the dimension of the valve need to be carefully designed to maximize the passive capability of the system. For severe sea state, bigger tanks are necessary to provide enough maximum counter torque. Larger lever arms also provide greater torque without occupying extra space onboard. The catamaran in this example is designed for offshore windmill installations, motivating the greater breadth and low speed. The system studied in this paper is suitable for similar working conditions such as offshore heavy lifting and anchor handling, etc. In special cases, the existing ballast water tanks can be modified into the proposed N-tank without significant structural modification.

Conclusion

This paper demonstrates a dynamic simulation scheme of an active roll reduction system using free-flooding tanks controlled by vacuum pumps. The system is using free-flooding tanks on ship sides which are open to the sea without air duct in between. Vacuum pumps with active stabilization controller provides optimal filling in these tanks based on input from the ship movement. The ship is simulated as a dynamic model with a single degree of freedom in roll. A control design model is derived for the vacuum pumps. The stability is proved by Lapunov's direct method and LaSalle-Yoshizawa theorem. For vessels which operate mostly at low speed and a relatively calm sea state, the system provides great performance with minor cost. Bigger tank is required for severe sea state. More detailed study about this design will be carried out with relevant companies.

Acknowledgement

This research is supported by Marine Roll & Pitch Control AS. Similar designs from this company have been employed on multiple vessels. This research is also partly funded by the

Research Council of Norway (RCN) project no. 237929: CRI MOVE, and partly by RCN project no. 223254: CoE NTNU AMOS.

REFERENCES

- [1] Moaleji, R., and Greig, A. R., 2005. "On the development of ship anti-roll tanks". *Ocean Engineering*, pp. 103–121.
- [2] Marzouk, O. A., and Nayfeh, A. H., 2009. "Control of ship roll using passive and active anti-roll tanks". *Ocean Engineering*, *36*, pp. 661–671.
- [3] Vasta, J., Gidding, A., Taplin, A., and Stilwell, J., 1961. "Roll stabilization by means of passive tanks". *Transactions of Society of Naval Architects and marine Engineers*, 69, p. 411.
- [4] Bell, J., and Walker, P., 1966. "Activated and passive controlled fluid tank system for ship stabilization". *Transactions of Society of Naval Architects and Marine Engineers*, 74, p. 150.
- [5] Frahm, H., 1911. "Results of trails of the anti-rolling tanks at sea". *Transactions of Institution of Naval Architects*, *53*, p. 183.
- [6] Halse, K. H., Asoy, V., and Sporsheim, O., 2012. "An actice roll reduction system using free flooding tanks controlled by vacuum pumps". In World Maritime Technology Conference.
- [7] Moaleji, R., 2006. "Adaptive control for ship roll stabilization using anti-roll tanks". PhD thesis, University College London
- [8] AMERICAN SOCIETY OF MECHANICAL ENGINEERS (ASME), 2001. Measurement of fluid flow using small bore precision orifice meters.
- [9] Cummins, W., 1962. The impulse response function and ship motions. Tech. Rep. 1661, SKIPSTEKNISK FORSKNINGSINSTITUTT.
- [10] Fossen, T. I., 2011. *Handbook of Marine Craft Hydrodynamics and Motion Control*. Wiley, Trondheim, Norway.
- [11] Nikiforov, V., 1998. "Adaptive non-linear tracking with complete compensation of unknown disturbances". *European journal of control*, *4*(2), pp. 132–139.
- [12] French, M., Szepesvári, C., and Rogers, E., 2003. *Performance of nonlinear approximate adaptive controllers*. John Wiley & Sons.
- [13] Khalil, H. K., and Grizzle, J., 1996. *Nonlinear systems*, Vol. 3. Prentice hall New Jersey.
- [14] Skjetne, R., and Fossen, T. I., 2004. "On integral control in backstepping: Analysis of different techniques". In American Control Conference, 2004. Proceedings of the 2004, Vol. 2, IEEE, pp. 1899–1904.